J Mater Sci: Mater Med (2007) 18:493–500
DOI 10.1007/s10856-007-2009-x

Biocompatibility of diamond-like nanocomposite thin films

T. Das · D. Ghosh · T. K. Bhattacharyya · T. K. Maiti

Received: 14 May 2005 / Accepted: 24 October 2005

Abstract Diamond-like nanocomposite (DLN) films consist of network structure of amorphous carbon and quartz like silicon. In the present work, DLN films have been synthesized on pyrex glass and subsequently, their biocompatibility have been investigated through primary and secondary cell adhesion, cytotoxicity, protein adsorption and murine peritoneal macrophage activation experiments. Variable degree of cell and protein response have been found based on variable film synthesis parameters but in overall, required biocompatibility has been established for all types of film-coating.

1 Introduction

Amorphous "Diamond-like" carbon composites (aC:H), with a number of unique bulk and surface properties, constitute a novel class of diamond related materials [1–4]. Diamond-like Carbon (DLC) films, by virtue of their excellent mechanochemical properties, are highly promising for cutting and forming applications, especially for processing non-ferrous and hard to machine materials [5–9]. Parallel to the exposure of its advantageous mechanical properties, DLC coating is gaining utilities in fabrication of biomedical devices for its low friction coefficient, high hardness, smooth finish and chemical inertness [1]. DLC has found major applications in fabrication of vascular stent coatings [10–12], hip prostheses [13–18], orthopaedic implant alloys and artificial heart diaphragm [19]. Studies clearly show that use of DLC film coating on artificial hip joints reduces the wear by a significant magnitude [13–18]. Thus having such a vibrant prospect of biomedical uses, for years DLC films have been subjected to various biocompatibility verifications: (a) the morphological behavior, adhesion and growth of osteoblast [20–22]; (b) platelet attachment and activation [23–26]; (c) haemocompatibility evaluation [27]; (d) Adhesion, cytoskeletal architecture and activation status of primary human macrophages [11, 28]; (e) *in vitro* cytocompatibility studies [29]; (f) protein adsorption studies [26]; (g) long term tissue response [30] and (h) other general biocompatibility studies [31].

One of the emerging classes of the modified DLC coating is Diamond-like nanocomposite (DLN) that is surging through multifarious upcoming industrial applications. Amorphous carbon (or Diamond-like) films are generally regarded as a mixture of sp^3 and sp^2 bonded carbon [1]. The DLN films mainly consist of Diamond-like aC:H and quartz-like aSi:O networks. Distinguishing features of DLN that immediately attracts over DLC, is its low wear, less friction compared to DLC films and its non-hygroscopic nature [1–3]. However, in addition to the mechanical properties or physical properties, prior to any biomedical use, the biological performance of the material has to be characterized with respect to undesirable inflammation or infection due to adhesion of proteins, cells and bacteria to the active surface of the material [32]. *In vivo* initial adhesion of the protein molecules from body-fluid to the implant material largely facilitates bacterial adhesion while its mechanochemical behavior remains almost unchanged. Though De Scheerder *et al*. has reported biocompatibility of Diamond-like nanocomposite (DLN) stent coatings in porcine coronary stent model [33], but to the best of our knowledge, no experiment has been performed to characterize cytotoxicity, protein adsorption or

T. Das · D. Ghosh · T. K. Maiti (✉)
Department of Biotechnology, Indian Institute of Technology, Kharagpur, India
e-mail: tkmaiti@hijli.iitkgp.ernet.in

T. K. Bhattacharyya
Department of Electronics and Electrical Communication Engineering, Indian Institute of Technology, Kharagpur, India

macrophage adhesion property of this novel material. We have synthesized a novel DLN film on Pyrex Glass and evaluated its cytotoxicity, fibroblast and macrophage adhesion and protein adsorption to the material in order to ascertain its fitness for biomedical implant devices.

2 Materials and methods

2.1 Materials

DLN thin films on glass surface were used as sample 0803011 and 2407991 (code numbers were given as per manufacturing conditions of DLN films on the surface of Pyrex Glass slides which were kept as substrate). Glass slides (Pathology Brand) have been used as control.

For maintaining L929 mice fibroblast cell line, Dulbecco's Modification of Eagle's Medium (DMEM) from HIMEDIA, supplemented with 10% fetal bovine serum (FBS), have been used while murine splenocytes and peritoneal macrophages were cultured in RPMI 1640 medium (HIMEDIA). For peritoneal Macrophage isolation, Swiss Albino mice of 6–8 weeks of age-groups have been selected. Each of the experiments has been done in triplicate with five readings taken per average data.

In protein adsorption, fetal bovine serum (HIMEDIA) has been utilized.

2.2 Film synthesis

Diamond-like nanocomposite thin films had been deposited via proprietary plasma enhanced chemical vapor deposition process. Substrate (Pyrex glass slides) was cleaned in an ultrasonic bath using Trichloroethylene (TCE) as well as acetone. Afterwards it was cleaned by methanol also in ultrasonic bath. The sample was then rinsed in De-ionized water and dried by the nitrogen gas. Further substrates were cleaned *in situ* by argon-plasma etching prior to deposition. DC discharge plasma, using a hot filament was created which fragments and ionizes siloxane or silazane based precursors or their combinations. The siloxane/silazane was mixed in different proportions in liquid form and dispensed in the plasma chamber. Consequently, for synthesis of the sample 2407991, pure Siloxane precursor was used while deposition was carried out in Argon-Methane ambience; whereas deposition of thin film in the sample 0803011 involved dispension of a mixed precursor (Siloxane:Silazane::70:30) composition in a argon-rich inert environment. The ratio of the Siloxane and Silazane influences the film property and composition. While depositing the thin film over the substrate, it is suitably biased by DC as well as RF voltages. A substrate temperature was kept around 250°C by using or by flowing cold water through the substrate holder assembly. The arrangement was to provide a planetary motion to the substrate holder plate in order to ensure uniform thickness of the film. The growth rate was maintained at 1 μm per hour. Deposition parameters were maintained as follows: (1). Chamber pressure during film growth $\approx 4 \times 10^{-4}$ Torr, (2). Substrate holder potential $\approx$500 V, (3). RF Power $\approx 2 \times 10^{3}$ Wm^{-2}. Here, biocompatibility tests were carried on two samples, named as 0803011 and 2407991. The difference between two samples lies in the composition of the precursors. Change in the composition of precursor effects carbon to silicon ratio, implying that the sample 2407991 has greater carbon percentage compared to the sample 0803011.

Surface wettability were evaluated by measuring the static contact angle between 2 μl waterdrop and the surface by Contact angle Goniometer.

Surface roughness profiles for both of the samples were graphically analyzed using DEKTEK3 (Veeco^{TM})—surface profile measuring system (Version 2.12). Important parameters used during the runs are described below: (a) Scan Speed—Low (25 s), (b) Data points—1000, (c) Measuring Range—655 KA, (d) Profiles—Hills & Valleys.

2.3 Cell adhesion and morphology studies

These studies have been carried out with mouse splenocytes and L929 mouse fibroblast cell line. In each of the investigations, three discs of each of the DLN samples were equilibrated with phosphate buffered saline (PBS) overnight in 35 mm petriplates (Tarson). Discs were incubated with 10^6 cells/ml at 37°C and 5% CO_2 for 48 h in appropriate media. Cells suspension was aspirated off and discs were rinsed twice with PBS. Discs containing adhered cells were then stained with Trypan blue in order to distinguish the viable cells from the non-viable ones. Stained discs were then washed with PBS to remove excess of the dye, placed under a light microscope and viable-cell counts were taken for each of the 5 fields on each disc at 10X magnification.

2.4 Evaluation of cytotoxicity

Sample and glass (treated as the "blank") discs were thoroughly washed with dehydrated alcohol and subsequently Ultra Violet (UV) *sterilized* for 1 h to ensure absence of any contamination. They were rinsed thrice with complete DMEM medium under sterilized condition. A cultured L929 cell line was centrifuged at 1000 rpm for 10 min, supernatant was discarded and the cell pellet was diluted in complete DMEM medium. Final cell concentration was adjusted to 10^5 cells/ml. 20 μl of the cell suspension was placed in each of discs, kept in 35 mm disposable petriplates (Tarson) and incubated at 37°C for one hour to facilitate adhesion of the cells to the surface of samples as well as the glass slide. Then, 3 ml of complete DMEM medium was added to each

of the petriplates and again incubated at 37°C and 5% CO_2 in totally sterile environment.

One of each of the samples and one blank were taken out after 24, 48 and 72 h of incubation. Each time, a standard colorimetric MTT ((3-(4,5-dimethylthiazol-2-yl)-2,5-diphenyl tetrasodium bromide) assay were performed. For each of discs, after 4 h of treatment with MTT, supernatants were Discarded, formazan crystals were dissolved in Dimethylsulphoxide (DMSO) and absorbance was measured with the test wave-length of 570 nm in a spectrophotometer [34].

2.5 Protein adsorption studies

The DLN coated sample 0803011, 2407991 and control discs (glass slides) were incubated with 2% FBS for 2 h at 37°C. FBS was removed and samples were transferred to 35 mm disposable petriplates (Tarson), washed with PBS for 30 min, with gentle agitation. The samples were transferred to new petriplates and incubated with Laemmli sample buffer for 1 h at 37°C. The sample buffer was removed from each of the samples, and subsequently stored in different mini-eppendorf tubes at 4°C. The samples were washed thrice with PBS and transferred again to new petriplates. Samples were incubated with 1% trichloroacetic acid (TCA) at 37°C for 1 h. The TCA was removed from each sample individually and the recovered TCA was stored in individual mini eppendorf tubes at 4°C. A 10% separating gel and an upper stacking SDS PAGE gel were prepared. 20 μl of each sample was loaded into individual wells in the gel, and the gel was run at 120 V for 120 min. FBS sample was run along side, with 20 μl was added to 5 μl of sample buffer. BSA was run along side as the molecular weight marker.

After completion of the electrophoresis, gel was fixed using a fixative solution (50% Methanol, 12% Acetic Acid, 37% Formaldehyde 0.05%) for minimum 1 h with gentle agitation. Fixed gel was stained by Silver-staining method.

2.6 Peritoneal macrophage adhesion studies

Macrophages were isolated by injecting autoclaved and membrane filtered ice cold PBS into mouse peritoneal cavity and subsequently withdrawing it. Isolated fluid was then treated with complete RPMI medium and centrifuged at 1000 rpm for 10 min. After centrifugation, layer of the mononuclear cells was diluted with complete RPMI medium and the final cell concentration was adjusted to 5×10^5 cells/ml. 75 μl droplets were then put onto each of the two samples were the control discs and incubated at 37°C and 5% CO_2 for one hour under proper sterile condition in 25 mm UV-irradiated petriplates. Discs were washed thrice with PBS; the adhered cells were fixed to the surface of the each disc with 4% Paraformaldehyde for 20 min in room temperature and washed thrice in excess of PBS. Adhered cells were subsequently permeabilised with 0.2% v/v Triton X-100 in PBS, for 8 min at room temperature and washed thrice in PBS. Adherent cells were stained with Propidium iodide and washed thrice to remove excess of the dye. Discs were then observed under a fluorescent microscope on 10X magnification and counts were taken for each of the 10 fields on each of the discs.

2.7 Peritoneal macrophage activation tests

Murine resident peritoneal cells were isolated by a similar procedure as described in case of macrophage adhesion studies in section 2.6. The final cell concentration was adjusted to 2×10^7 cells/ml. Two hundred microlitre droplets were then placed onto each of the discs in 25 mm UV-irradiated petriplates and incubated at 37°C and 5% CO_2 for 1 h under proper sterile condition and subsequently 1 ml of complete RPMI was added to each of the samples and the blank. Final cell concentration was thus adjusted to 4×10^6 cells/ml. For each of the experiments, two copies of blank and sample were kept. One of two replicates, for each of the cases considered, were incubated with Concanavalin A (ConA) solution that served as a positive control. After one day incubation of all the replicates at 37°C and 5% CO_2, 250 μl medium was pipetted out and stored in eppendorf tubes. Two hundred and fifty microlitre of each of the components of Griess reagent solution were added to the recovered medium and absorbance readings were taken at 550 nm.

3 Results

3.1 Material synthesis

Mechanochemical characteristics of the films were examined by the following methods: (a) Adhesion of the film was tested by Scotch Tape and it was found that the thin film layer could not be removed by this method; (b) Films were treated with heated air (100°C for 24 h) as well as with inert atmosphere in nitrogen gas filled chamber (25°C for 24 h) and exhibited notable thermal stability in oxidizing as well as non-oxidizing environment and its physical properties were unaltered up to 500°C; (c) Synthesized films were treated with Piranha solution (H_2SO_4:H_2O_2::3:1 v/v) for 1 h at 25°C; with 2M Sodium hydroxide solution at pre-boiling condition (80°C) for 1 h and were found to be resistant to acid or alkali mediated degradation; (d) The film hardness was obtained at the applied load of 2 mN in the measurement of the ultra micro-indentation system [1] and the hardness of DLN films were found to 15, 22 GPa with different deposition conditions i.e. for the sample 0803011 and the sample 2407991, respectively; (e) The film also exhibited low co-efficient of friction (0.01) which was even lower than the experimental results obtained by

Yang *et al*. [1], (f). Tailorable surface energy and Contact angle of the film were measured to be $2-4\times10^{-2}$ N/m and 70–100° (by Contact Angle Goniometer), respectively, which was in agreement with wettability measured by Nurdin *et al*. [27].

Surface analysis by DEKTEK3—Surface Profile Measuring system exhibited a comparatively rougher surface in case of the sample 2407991 (Figs. 1.1 and 1.2). While surface roughness of the sample 0803011 ranges approximately 50 Å and evidently quite uniform in nature; surface of the sample 2407991 was found be of great variability, in places variation could be as large as 200 Å. After the initial scan, profiles were automatically leveled by the integrated software system and Average Step Height (ASH) and slope were calculated. For the sample 2407991: ASH = 439.659 Å and Slope = −59.855 mdg; while for the sample 0803011: ASH = 40.180 Å and Slope = −9.929 mdg. Hence, greater surface roughness of the sample 2407991 in comparison to that of the sample 0803011 could be manifested in the results.

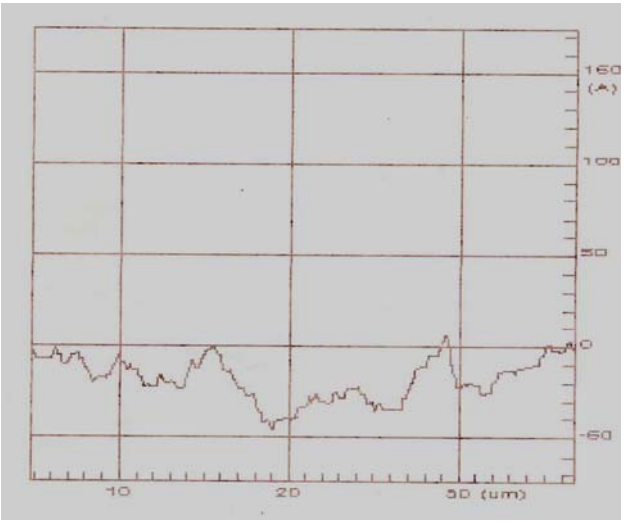

Fig. 1. 1 Surface Roughness profile of the Sample 0803011 as measured by DEKTAK 3.

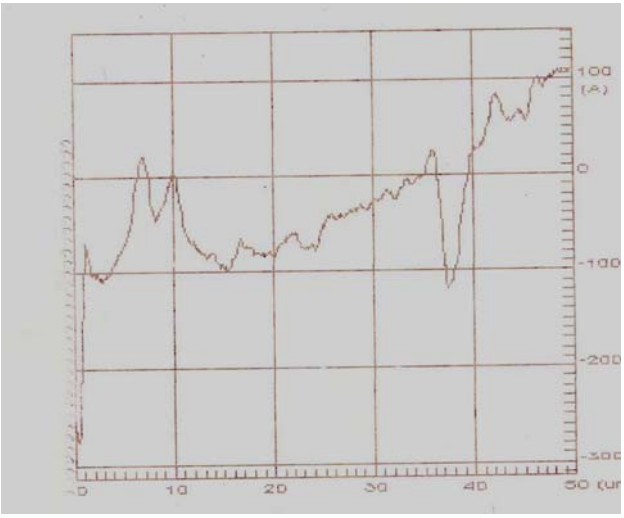

Fig. 1. 2 Surface Roughness profile of the Sample 2407991 as measured by DEKTAK 3.

3.2 Cell adhesion and morphology studies

In order to compare between two DLN coated thin films i.e. sample 0803011 and 2407991, statistical analysis was carried out using two-sample *t*-test. In case of L929, mouse fibroblast cell line and splenocytes (Figs. 2.1 and 2.2), number of adherent cells on sample 0803011 was found to be less than that on sample 2407991 ($p < 0.05$). Also, significant differences of number of adherent cells were observed while adhesion to sample 2407991 and the control was compared for both of the cell lines (Figs. 2.1 and 2.2, $p < 0.05$). There was no evidence of material toxicity found for any of the materials considered; neither any evidence of necrotic cells on the

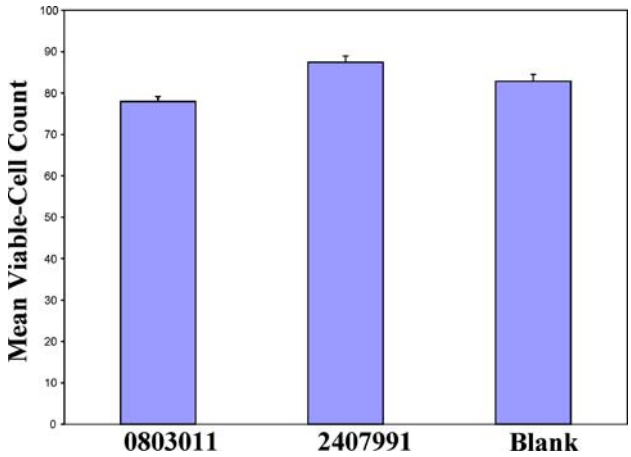

Fig. 2. 1 L929 Mouse Fibroblast adhesion to the materials incubated with approximately 10^6 cells after 48 h. Mean ± SEM. $p < 0.05$.

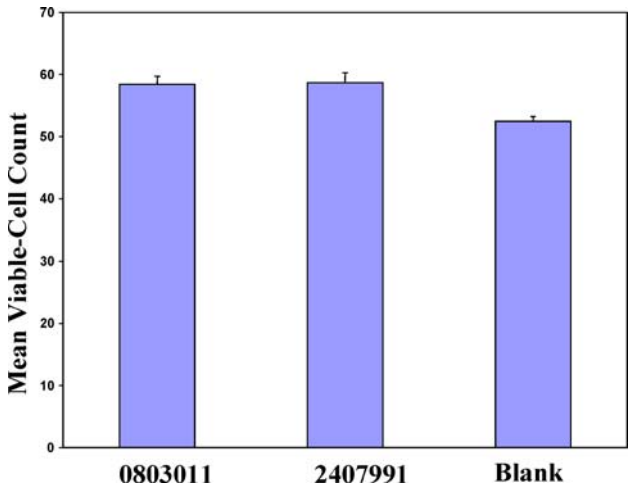

Fig. 2. 2 Splenocytes adhesion to the materials incubated with approximately 10^6 cells after 48 h. Mean ± SEM. $p < 0.05$.

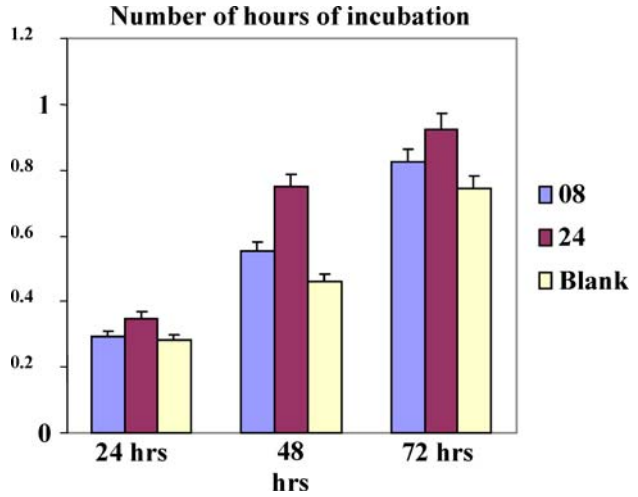

Fig. 3 MTT assay estimating the viable cell amount for the evaluation of cytotoxicity of the materials using L929 mouse fibroblast cells. Initial concentration is 10^5 cells/ml. All the readings were taken at 570 nm. 08–0803011, 24–2407991.

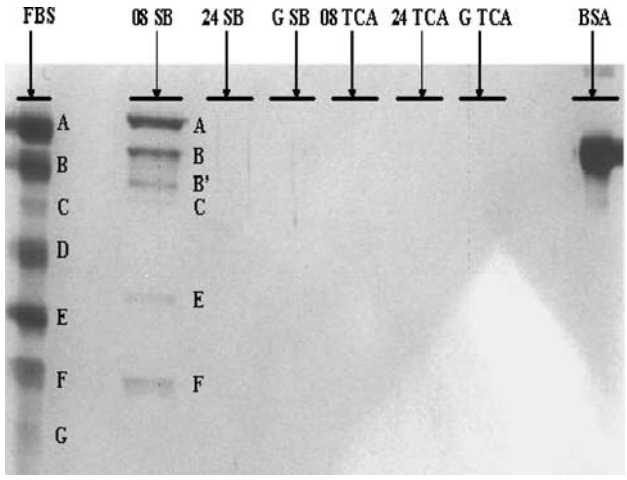

Fig. 4 10% SDS-PAGE photograph showing FBS adsorption on G: Glass, 08: 0803011, 24: 2407991 disc surfaces. SB and TCA represent protein extraction with sample buffer and Trichloroacetic acid respectively.

surface of the materials was observed. No abnormal change in morphology of any of the cell lines was be detected.

3.3 Evaluation of cytotoxicity

Uniform growth pattern was observed for all of the materials, with no evidence of toxicity of any of the materials being depicted. However, growth of the L929 mouse fibroblast cells on the sample 2407991 was found to be significantly more (Fig. 3; $p < 0.05$) for all of the readings taken at 24, 48 and 72 h of incubations. Before performing the MTT colorimetric assay for cell viability, each of the discs were scrutinized under a light microscope. Mouse fibroblast cells were observed to grow on the surface of the discs and no evidence of necrotic cell death was found.

3.4 Protein adsorption studies

In order to facilitate individual analysis of protein bands, we named each of distinguishable bands of FBS in alphabetical order down the gel-lane i.e. in decreasing order of molecular weight. Though, this method is hundred percent correct as far as the qualitative comparisons are concerned, quantitative distinctions of the banding patterns, hence the adsorption patterns, can well be established and confirmed, repeating the experimental method several times. From SDS-PAGE gel electrophoresis data (Fig. 4), extraction of protein with sample buffer and TCA from the surfaces of sample 2407991 and the glass (similar results as compared to the data published by S. L. West *et al*. [32]) did not show any band. Extraction of adsorbed protein with TCA from 0803011-disc surface also displayed similar results. However, extraction with sample buffer from the sample 0803011 depicted visible bands repeatedly. But E, F bands of the extraction was observed to be less intensive compared to A, B bands whereas, in case of FBS-lane, all the bands were found be in almost same intensities. Presence of an extra band B′ and absence of band D in the extraction were also noticeable features of observation.

3.5 Peritoneal macrophage adhesion studies

In statistical analysis of macrophage adhesion onto the surface of the samples and the glass slide, mean number of adhering macrophages was observed to be approximately similar (Fig. 5). Though number of the cells attached to the surface of the sample 0803011 appeared to be less while compared to the number of cells attached to 2407991, significance of

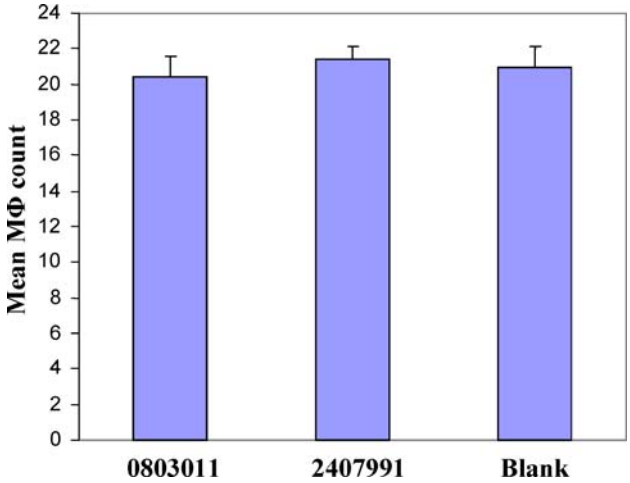

Fig. 5 Macrophage adhesion to the materials incubated with approximately 5×10^5 cells after one hour of incubation. Mean ± SEM. $p < 0.05$.

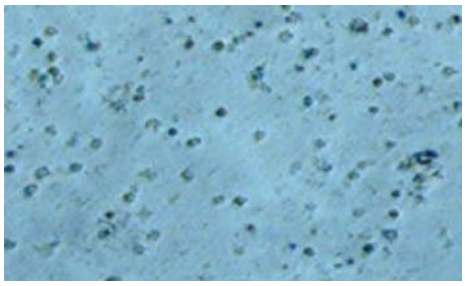

Fig. 6. 1 Murine Peritoneal Macrophage adhesion to the sample 0803011 in 20X view.

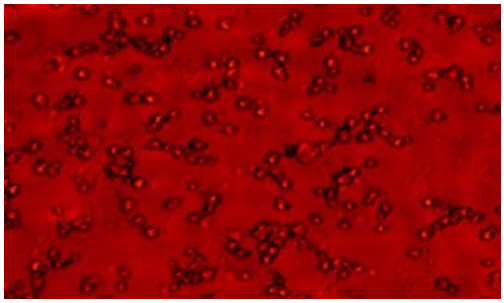

Fig. 6. 2 Murine Peritoneal Macrophage adhesion to the sample 2407991 in 20X view.

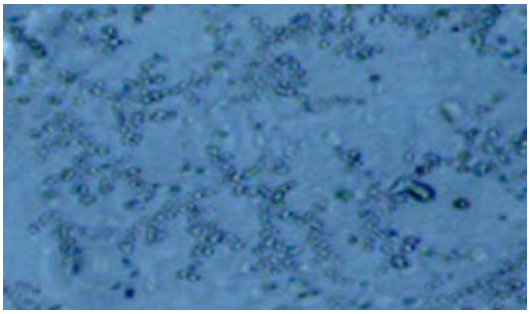

Fig. 6. 3 Murine Peritoneal Macrophage adhesion to the Glass Slide in 20X view.

this result could not be established from statistical analysis ($p > 0.05$). Neither any morphological change nor any kind of toxic effect to of the adherent cells could be detected for all cases under consideration. As indicated by the 20X magnification of adhered macrophage in 0803011, 2407991 and glass surface in Figs. 6.1, 6.2 and 6.3 respectively.

3.6 Peritoneal macrophage activation tests

The relation between macrophage cytotoxicity and enhanced production of reactive nitrogen and oxygen intermediates is well known. Elevated levels of inorganic nitrite (NO_2^-) formed in culture medium from cytokine-activated macrophages. NO_2^- is a stable oxidative end product of the antimicrobial effector molecule nitric oxide. Activated macrophages catalyze the oxidation of one of the two chemically equivalent guanidino nitrogens of L-arginine to nitric oxide which in turn, in presence of oxygen and water, reacts

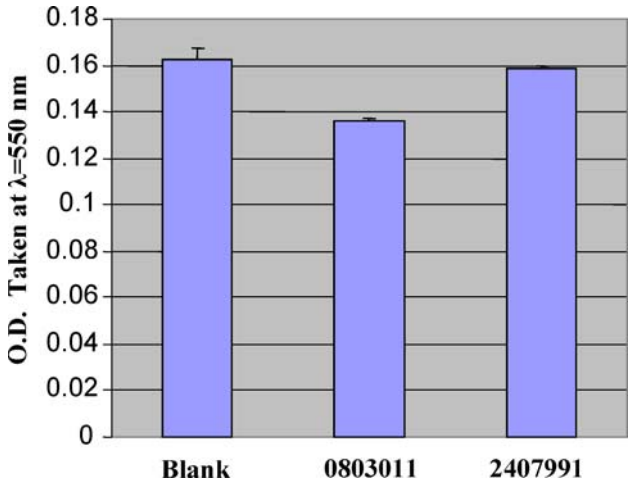

Fig. 7 Murine Peritoneal Macrophage activation study to the materials incubated with approximately 2×10^7 cells. Mean ± SEM. (Activated with Concanavalin A).

with itself to produce other nitrogen-oxide intermediates including NO_2^-. Results obtained (Fig. 7) clearly shows that level of production of NO_2^- by ConA activated macrophages is statistically lower in case of the sample 0803011 in comparison to either of the sample 2407991 or the blank. In contrast, NO_2^- synthesis in ConA activated sample 2407991 was quite comparable with that in blank surface. However similarity in the level of NO_2^- generation was evident in all the samples and the glass without any treatment with ConA.

4 Discussion

The aspect of using DLC in fabrication of Micro electro mechanical systems (MEMS) such as Micromotors was earlier highlighted by Beerschwinger *et al*. as the wear rate of DLC and single-crystal silicon sliding on DLC was shown to be decreasing with increasing sliding distance [7] whereas Diamond-like a novel surface acoustic wave (SAW) filter, manufactured by evaporating interdigital transducers on ZnO thin films was successfully implemented by Tang *et al*. [8]. Recently, solid mechanical performance, anti-corrosion behavior [6] and tribological characteristics [9] of the DLC films were investigated by various researchers. In parallel, DLC films have been tested for their biocompatibility by numerous research groups, which have enabled DLC compounds to achieve a widespread use in the field of Biomedical Engineering as vascular stent coatings, hip prostheses, orthopaedic implant alloys and artificial heart diaphragm. Notable among the virtues of the DLC films, those are responsible for its shear acceptability as a biomaterial are its low wear during in contact with physiological environment and inherent low friction. However it has been a well-established fact that considering the properties mentioned above DLN is a superior material in comparison to DLC [1]. Following the works of Yan *et al*., the Diamond-like nanocomposite (DLN)

films composed of an amorphous carbon network (aC:H) and amorphous silica network (aSi:O) are of a great significance because of their excellent adhesion to various substrate materials (i.e., metals, plastics, ceramics, semiconductors, etc.), high hardness, low internal residual stress, excellent thermal stability, and excellent wear resistance. Thus they have significant advances over the conventional DLC films [3] but their applications have been limited owing to the complicated and costly equipment and rigorous preparation conditions usually by various chemical and physical vapor deposition techniques such as ion beam assisted deposition, multicascade remote plasma vacuum deposition, inductively coupled plasma CVD. Quite recently, cost of manufacturing Diamond-like nanocomposite films have been cut down by the introduction of liquid or electrochemical deposition techniques [3]. This has definitely increased DLN films practical utility by an enormous magnitude. Although the mechanochemical behaviors of the Diamond-like nanocomposite thin films have been well characterized, there exists a visible dearth of literatures investigating its biocompatibility. This encourages us to look into the overall biocompatibility of Diamond-like nanocomposite films.

Three important studies—(a) Cell adhesion and morphological characterization, (b) Cytotoxicity test and (c) Macrophage adhesion test show overall preferential cell adhesion to the sample 2407991 over the sample 0803011 or the glass slide (blank) and can have several implications. In many biomedical applications, the adhesion of cells to biomaterials causes undesirable inflammation or infection and various groups have, therefore, focused on the development of bioinert, biocompatible coatings which can be used to minimize protein adsorption and cellular adhesion whilst maintaining the mechanical and physical properties of the underlying substrate [32]. However, when used as Bioactive material, increased cell adhesion can, in contrast to the drawback previously stated, facilitate increased biocompatibility for those applications. Significantly, from our studies, it can be stressfully commented that by varying the process parameters and the ratio of the precursor compositions one can achieve variable degree of cell adhesion or protein adsorption leading to its multiplicative flexibility for the utilization in biomedical applications. Although apparently the splenocytes and L929 cell data (Figs. 2.1 and 2.2) shows a lower cell adhesion to the sample 0803011 in comparison to the sample 2407991, favored adhesion of cells on the surface of the sample 2407991 could help the nanocomposite coating on artificial stents (an area where DLC has gained its popularity and frequent use as a biomaterial) to undergo a proper endothelialisation [32]. With respect to the surface roughness data, preferential cell adhesion on to the sample 2407991 can be attributed to its greater variability in surface texture and roughness as compared to the relatively smooth surface of the sample 0803011. The most important governing factor for the successful use of an implant is a good adhesion of the surrounding tissue to the biomaterial. In addition to the surface composition of the implant, the surface topography and roughness also influence the properties of the adherent cells [35]. It has been well known that fibroblasts intrinsically respond to the microtopography of the substratum surface, a phenomenon termed ‘contact guidance’ meaning the alignment of the cell in relation to the microstructures of the substratum surface. Preceding studies have elaborately shown a positive correlation between the surface roughness and fibroblast adhesion in various inorganic substrates such as titanium, titanium alloys, calcinated metal surfaces etc. [35–37]. This study efficiently puts forward a reasonably firm agreement with anticipated results in case of Diamond-like nanocomposite thin films.

Macrophage activation study exhibits a normal activation of inflammatory cells, implicating a matching even reduced inflammatory response while compared to glass slides. The sample 0803011 is less likely to initiate an inflammatory response than the sample 2407991 coating. Two main causes could be responsible for the differential nitric oxide activity of the macrophages adhered to the films and the control surface (a) preferential adhesion of peritoneal macrophage cells on one surface than the other i.e. more number of adhering macrophages incites more nitric oxide liberation; (b) surface characteristics i.e. differential adsorption, denaturation, ligation of the protein on the surface could be counted for distinguishable differences in nitric oxide liberation [32]. However, in the present study, difference in the number of macrophage adhering to the surface of the two DLN films are low enough (Fig. 5) to effect such difference in the macrophage activity. In fact Fig. 5 shows difference of only 1-2 cells per field view of the microscope. Hence, differential macrophage activity can be attributed to the surface characteristics of the two DLN films. Micromotion at the interface leading to cellular damage probably causes the production of a soft tissue capsule and also induces local inflammation [38]. In an exhaustive study, relating macrophage responses to the surface properties of microtextured silicone, it was concluded that cells were influenced by the size of the events and the roughness of the surfaces more than any other variables [39]. A quite similar argument holds sufficiently well for the inferences of the present study.

Subsequently, protein adhesion study to the materials implicates that the sample 0803011 has all the characteristic bands of fetal bovine serum while the sample 2407991 does not give any visible output. These results may support the view that differential denaturation, adsorption, and ligation of plasma proteins occurs on different substrates. Protein adhesion is important in initial conditioning of the material when it is implanted into the body and is instrumental in activation of various inflammatory cascades and in providing adhesion sites for some bacteria on particular substrates.

The fact that proteins are found associated with the sample 0803011 surface but do not give rise to excessive inflammatory cell adhesion may suggest that these proteins may exist in their native conformation [32] retention of which may be facilitated by the relatively smooth surface micro-architecture of the sample. Evidently plasma proteins have multiple effects on the biocompatibility of different substrates that is probably determined by the ability of a particular surface to adsorb, denature and enhance ligation of particular plasma proteins. It can likely be stated that the most effective biocompatible surface will be the surface on which associated proteins are retained in their native conformation. It should however be noted that care must be taken to ensure that these nanocomposite thin film coatings do not crack or delaminate on handling as exposure of the underlying substrate at cracked interfaces clearly provides a niche for inflammatory cell adhesion. Clearly there is a need to ensure that coatings are suitably pliable to withstand any handling or flexing of the device on insertion. Moreover, the results of the cytotoxicity test that clearly manifests the absolute absence of any necrotic cell death, strengthening the qualification of both the samples as a biocompatible material.

References

1. W. J. YANG, Y. H. CHOA, T. SEKINO, K. B. SHIM, K. NIIHARA and K. H. AUH, *Mater. Lett.* **57** (2003) 3305.
2. C. CHEN and F. C. HONG, *Appl. Surf. Sci.* **242** (2005) 261.
3. X. YAN, T. XU, G. CHEN, Q. XUE and S. YANG, *Electrochem. Commun.* **6** (2004) 1159.
4. L. CHEN and F. C. HONG, *Appl. Phys. Lett.* **82** (2003) 3526.
5. C. CHANG and D. WANG, *Diamond Relat. Mater.* **10** (2001) 1528.
6. G. F. HUANG, Z. LINGPING, H. WEIQING, Z. LIHUA, L. SHAOLU and L. DEYI, *Diamond Relat. Mater.* **12** (2003) 1406.
7. U. BEERSCHWINGER, T. ALBRECHT, D. MATHIESON, R. L. REUBEN, S. J. YANG and M. TAGHIZADEH, *Wear* **181–183** (1995) 426.
8. I. TANG, H. CHEN, W. C. HWANG, Y. C. WANG, M. HOUNG and Y. WANG, *J. Cryst. Growth* **262** (2004) 461.
9. M. BAN, M. RYOJI, S. FUJII and J. FUJIOKA, *Wear* **253** (2002) 331.
10. M. SANTIN, L. MIKHALOVSKA, A. W. LLOYD, S. MIKHALOVSKY, L. SIGFRID, S. P. DENYER, S. FIELD and D. TEER, *J. Mater. Sci. Mater. Med.* **15** (2004) 473.
11. M. BALL, A. O′BRIEN, F. DOLAN, G. ABBAS and J. A. MCLAUGHLIN, *J. Biomed. Mater.* **70A** (2004) 380.
12. F. AIROLDI, A. COLOMBO, D. TAVANO, G. STANKOVIC, S. KLUGMANN, V. PAOLILLO, E. BONIZZONI, C. BRIGUORI, M. CARLINO, M. MONTORFANO, F. LIISTRO, A. CASTELLI, A. FERRARI, F. SGURA and C. DI MARIO, *Am. J. Cardiol.* **93** (2004) 474.
13. J. FISHER, X. Q. HU, T. D. STEWART, S. WILLIAMS, J. L. TIPPER, E. INGHAM, M. H. STONE, C. DAVIES, P. HATTO, J. BOLTON, M. RILEY, C. HARDAKER, G. H. ISAAC and G. BERRY, *J. Mater. Sci. Mater. Med.* **15** (2004) 225.
14. M. KIURU, E. ALAKOSKI, V. M. TIAINEN, R. LAPPALAINEN and A. ANTTILA, *J. Biomed. Mater. Res. B Appl. Biomater.* **66** (2003) 425.
15. S. SANTAVIRTA, *Acta Orthop. Scand. Suppl.* **74** (2003) 1.
16. J. FISHER, X. Q. HU, J. L. TIPPER, S. WILLIAMS, M. H. STONE, C. DAVIES, P. HATTO, J. BOLTON, M. RILEY, C. HARDAKER, G. H. ISAAC, G. BERRY and E. INGHAM, *Proc. Inst. Mech. Eng. [H]* **216** (2002) 219.
17. V. SAIKKO, T. AHLROOS, O. CALONIUS and J. KERANEN, *Biomaterials* **22** (2001) 1507.
18. S. C. SCHOLES, A. UNSWORTH and A. A. GOLDSMITH, *Phys. Med. Biol.* **45** (2000) 3721.
19. Y. OHGOE, S. TAKADA, K. K. HIRAKURI, K. TSUCHIMOTO, A. HOMMA, T. MIYAMATSU, T. SAITOU, G. FRIEDBACHER, E. TATSUMI, Y. TAENAKA and Y. FUKUI, *ASAIO J.* **49** (2003) 701.
20. R. KORNU, W. J. MALONEY, M. A. KELLY and R. L. SMITH, *J. Orthop. Res.* **14** (1996) 871.
21. C. DU, X. W. SU, F. Z. CUI and X. D. ZHU, *Biomaterials* **19** (1998) 651.
22. M. ALLEN, R. BUTTER, L. CHANDRA, A. LETTINGTON and N. RUSHTON, *Clin. Mater.* **17** (1994) 1.
23. P. YANG, N. HUANG, Y. X. LENG, J. Y. CHEN, R. K. FU, S. C. KWOK, Y. LENG and P. K. CHU, *Biomaterials* **24** (2003) 2821.
24. L. K. KRISHNAN, N. VARGHESE, C. V. MURALEEDHARAN, G. S. BHUVANESHWAR, F. DERANGERE, Y. SAMPEUR and R. SURYANARAYANAN, *Biomol. Eng.* **19** (2002) 251.
25. K. GUTENSOHN, C. BETHIYEN, J. BAU, T. FENNER, P. GREWE, R. KOESTER, K. PADMANABAN and P. KUEHNL, *Thromb. Res.* **99** (2000) 577.
26. M. I. JONES, I. R. MCCOLL, D. M. GRANT, K. G. PARKER and T. L. PARKER, *J. Biomed. Mater. Res.* **52** (2000) 413.
27. N. NURDIN, P. FRANCOIS, Y. MUGNIER, J. KRUMEICH, M. MORET, B. O. ARONSSON and P. DESCOUTS, *Eur. Cell Mater.* **5** (2003) 17.
28. S. LINDER, W. PINKOWSKI and M. AEPFELBACHER, *Biomaterials* **23** (2002) 767.
29. A. SINGH, G. EHTESHAMI, S. MASSIA, J. HE, R. G. STORER and RAUPP, *Biomaterials* **24** (2003) 5083.
30. M. MOHANTY, T. V. ANILKUMAR, P. V. MOHANAN, C. V. MURALEEDHARAN, G. S. BHUVANESHWAR, F. DERANGERE, Y. SAMPEUR and R. SURYANARAYANAN, *Biomol. Eng.* **19** (2002) 125.
31. L. A. THOMSON, F. C. LAW, N. RUSHTON and J. FRANKS, *Biomaterials* **12** (1991) 37.
32. S. L. WEST, J. P. SALVAGE, E. J. LOBB, S. P. ARMES, N. C. BILLINGHAM, A. L. LEWIS, G. W. HANLON and A. W. LLOYD, *Biomaterials* **25** (2004) 1195.
33. I. D. SCHEERDER, M. SZILARD, H. YANMING, X. B. PING, E. VERBEKEN, D. NEERINCK, E. DEMEYERE, W. COPPENS and F. VAN DE WARF, *J. Invasive Cardiol.* **12** (2000) 389.
34. T. MOSMANN, *J. Immunol. Methods* **65** (1983) 55.
35. E. EISENBARTH, J. MEYLE, W. NACHTIGALL and J. BREME, *Biomaterials* **17** (1996) 1399.
36. L. C. BAXTER, V. FRAUCHIGER, M. TEXTOR, I. GWYNN and R. G. RICHARDS, *Euro. Cells Mater.* **4** (2002) 1.
37. A. CITEAU, J. GUICHEUX, C. VINATIER, P. LAYROLLE, T. P. NGUYEN, P. PILET and G. DACULSI, *Biomaterials* **26** (2005) 157.
38. J. A. JANSEN, J. P. C. M. WAERDEN and K. GROOT, *J. Mater. Sci.: Mater. Med.* **1** (1990) 192.
39. J. A. SCHMIDT and A. F. VON RECUM, *Biomaterials* **13** (1992) 1059.